

Nano-film pesticide for *Schistosoma japonicum* cercariae: synthesis, characterization, toxicity and insecticidal effect†

Cite this: *RSC Adv.*, 2013, **3**, 19956

Received 13th August 2013
Accepted 2nd September 2013

DOI: 10.1039/c3ra44328k

www.rsc.org/advances

Yibao Li,^a Yunzhi Xie,^a Chunhua Liu,^a Wei Guo,^a Xiaokang Li,^a Xun Li,^a Qingdao Zeng^{*b} and Xiaolin Fan^{*a}

To improve the efficiency of pesticides, two novel niclosamide derivatives have been synthesized by adding polyethylene glycol groups (PEG) with different lengths to the niclosamide core. The derivatives were characterized by infrared spectroscopy (IR) and magnetic resonance (¹H NMR). The results from Brewster angle microscopy (BAM) revealed that these two derivatives formed a self-diffusion thin film at the air–water interface. In addition, Langmuir–Blodgett (LB) films on solid substrate have been used to investigate the formation mechanism of the thin film at the air–water interface, combined with atomic force microscopy (AFM). It was suggested that the height of the monolayer at the air–water interface is consistent with the theoretical length of niclosamide derivatives. Further experimental results indicated that these two compounds exhibit relatively low cytotoxicity to HeLa cells, but have higher efficiency to anti-cercariae compared with that of pristine pesticide.

1. Introduction

The cercarial stage of the schistosome life-cycle is the only infectious stage. The cercarial stage is also the most fragile stage in the life cycle of schistosome.¹ More than 98% of cercariae float on the water surface, so it is possible to effectively control the risk of cercariae infection by the use of a thin cercaricide film floated on the water.² Niclosamide (see Scheme 1, compound **1**) has a long track-record as a killer of the tapeworm and snails that harbor schistosome.³ Moreover, niclosamide can effectively prevent *Schistosoma japonicum* cercariae from entering a human host by rendering cercariae uninfected with very short contact time.⁴ Unfortunately, niclosamide has low

water solubility,^{5,6} so anti-cercarial effect of niclosamide is not good in actual application.

To improve the efficiency of pesticides, nano-film pesticide (derivatives of niclosamide) would be expected floating on the air–water interface. The development of nanomedicine might open up potential novel applications in agriculture and biotechnology,^{7–9} especially in biomedical and pharmacology.¹⁰ Besides it had low pollution to environment. Shi *et al.* had achieved nanomedicine for targeted drug delivery.¹¹ Zhang *et al.* had used nanospheres to prepare slow-release nanomedicine.¹² New opportunity and wide application prospect for the research on pesticide were provided by nanomedicine.

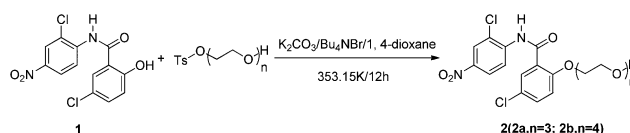
Due to the non-toxic and good biocompatibility, PEG has been approved by the FDA as intravitreal injection of medicinal polymer. The PEG polymers have many advantages: (1) solubility of the drug is increased, (2) half life enzymatic degradation is decreased, immunogenicity and period is prolonged, (3) maximum plasma concentration is lowered, the fluctuation of blood concentration is flattened, (4) antigenicity is reduced, toxicity is also reduced.^{13–18} Shen *et al.* had used PEG to improve solubility of the drug.¹⁹ Robinson *et al.* had used PEG to extend the half-life of nanomaterials *in vivo*.²⁰ In addition, Watkins *et al.* had used PEG to synthesise amphiphilic molecules which can self-diffuse at the water–air interface.²¹

Herein, this paper focuses on synthesis of novel niclosamide derivatives with PEG that can self-diffuse at the water–air interface, which will rapidly kill *S. japonicum* cercariae. Novel derivatives of niclosamide (Scheme 1, **2a** and **2b**) have been synthesized by coupling PEG with the niclosamide core. The film-forming ability of the novel niclosamide derivatives at the

^aKey Laboratory of Organo-Pharmaceutical Chemistry, Gannan Normal University, Ganzhou 341000, P. R. China. E-mail: Fanxl2013@gnnu.cn; Fax: +86 (0)797 8393536

^bNational Center for Nanoscience and Technology (NCNST), Beijing 100190, P. R. China. E-mail: zengqd@nanocn.cn; Fax: +86 (0)10 82545548

† Electronic supplementary information (ESI) available. See DOI: 10.1039/c3ra44328k



Scheme 1 The synthesis of **2** (**2a** and **2b**).

water–air interface was observed by the BAM. To further study the formation mechanism of film, LB technique has been used at the air–water interface, combined with AFM. In addition, the cell toxicity and anti-cercarial ability were further investigated.

2. Experimental section

2.1 Synthesis

2.1.1 2-[2-(2-Hydroxyethoxy)ethoxy]ethoxyl niclosamide (2a). **2a** was synthesized according to the literature procedure.^{22,23} Niclosamide (23.0 g, 70 mmol) was dissolved in 1,4-dioxane (100 mL) at 353.15 K in a 250 mL three-neck flask. K_2CO_3 (9.2 g, 70 mmol) and Bu_4NBr (2.30 g, 7 mmol) were added with stirring. 2-(2-(2-Hydroxyethoxy)ethoxy)ethyl 4-methylbenzenesulfonate (12.77 g, 42 mmol) dissolved in 1,4-dioxane (30 mL) was added dropwise and the ensuing mixture was heated under reflux for 12 h, and allowed to cool. Water (200 mL) was then added and the mixture was shaken in a separating funnel. The organic phase was separated, and the water phase extracted with CH_2Cl_2 (50×3 mL). The combined organic layer was dried over anhydrous Na_2SO_4 . After removing the solvent under reduced pressure, the crude product was purified by column chromatography, and a slightly yellow solid **2a** was obtained. Yield 79%. mp 84–86 °C IR (KBr) ν 3443, 3302(N–H, O–H), 3077, 2893(CH_2), 1673, 1592, 1542, 1509(Ar), 1402, 1340(N=O), 1271, 1207, 1118(C–O–C), 1048(Ar–Cl), 891, 827, 743(Ar), 675 cm^{-1} ; δ_H (400 MHz, $CDCl_3$) 10.62 (1H, s), 8.88 (1H, d, J 9.2), 8.35 (1H, d, J 2.6), 8.26 (1H, d, J 2.8), 8.23 (1H, dd, J 9.3, 2.6), 7.50 (1H, dd, J 8.9, 2.8), 7.11 (1H, d, J 8.9), 4.49 (2H, t, J 4.8), 3.96 (2H, t, J 4.8), 3.69–3.64 (4H, m), 3.60–3.57 (2H, m), 3.52 (2H, t, J 4.8). HR-MS: calcd for $C_{19}H_{20}Cl_2N_2O_7$: 459, $[M + H]^+$. Found: 459.

2.1.2 2-[2-(2-(2-Hydroxyethoxy)ethoxy)ethoxy]ethoxyl niclosamide (2b). The synthesis and separation methods for **2b** were similar to those adopted for **2a**, and a slight yellow liquid was obtained. Yield 70%. δ_H (400 MHz, $CDCl_3$) 10.58 (1H, s), 8.79 (1H, d, J 9.2), 8.27 (1H, dd, J 2.8), 8.17–8.11 (2H, m), 7.43 (1H, dd, J 8.9, 2.8), 7.08 (1H, d, J 8.9), 4.45 (2H, t, J 4.8), 3.92 (2H, t, J 4.8), 3.66 (2H, t, J 4.8), 3.64–3.61 (2H, m), 3.58–3.51 (8H, m), 2.79 (1H, s). MS: $[M + H]^+ m/z$ (%) 503.3.

2.2 BAM images of nano-film pesticides

Exploring the morphology of the film, the compounds **2a** and **2b** was investigated by this method in the following experiments. Compounds **2a** and **2b** was spread on the pure water surface with different concentration in chloroform. The film structure of the molecular was investigated by the BAM JB04 (POWER-EACH, Shanghai). The water was obtained from a pure water system.

2.3 Surface pressure–area (π -A) isotherms

The monolayers were formed by spreading a chloroform solution (1×10^{-3} mol L^{-1}) onto the surface of pure water. Surface pressure–area (π -A) isotherms were recorded on a KSV (KSV 1100, Finland) instrument with a compressing

speed of $7.5\text{ cm}^2\text{ min}^{-1}$ after waiting 20 min for the evaporation of the solvent.

2.4 AFM images of nano-film pesticides

The freshly cleaved mica plate was first immersed into the pure water. The compounds **2a** and **2b** in chloroform solutions were then spread on the sub-phase. After the spread film was compressed to a constant surface pressure (5, 10, 20 $mN\text{ m}^{-1}$) and waiting for 5 min for the equilibrium of the monolayer, the mica substrates were vertically lifted through the monolayer at a speed of 1 mm min^{-1} . Only one layer was transferred onto the mica surface, allowing the water to evaporate in air at room temperature. The mica was covered with watch glasses to protect their surfaces from dust. This may also help create a relatively confined space and make the evaporation of solvents slower as compared to that in an open-air environment. AFM measurements were performed by using a Nanoscope IIIa (Veeco Metrology, USA).

2.5 Toxicity test

The cell survival rates of **2a** and **2b** were detected by using MTT assay. HeLa cells were plated on 96 well tissue culture plate in an atmosphere of 5% CO_2 , 95% air at 37 °C to adhere for 12 h. Mixed the cell pellet with **2a** solution (100 μL per well), the final concentrations of 10, 20, 30, 40, 50, 60, 70, and 80 μM , the same procedure for **2b** and compound **1**, as experimental group. Mixed the cell pellet with RPMI 1640 medium containing 0.2% DMSO (100 μL per well), as reference group. After cell culture incubator for 24 h, added 20 μL of MTT/PBS (5 $mg\text{ mL}^{-1}$) to each well and cell culture incubator for 3 to 4 h. Remove culture medium, added 100 μL of DMSO to each well and measured the absorbance in each well, including the blanks, at 570 nm in a microtiter plate reader. The reference wavelength was 690 nm. The detail mathematical description of the cell survival rate is given by

$$\text{cell survival rate (\%)} = \left(\frac{\text{absorbance of experimental group}}{\text{absorbance of reference group}} \right) \times 100\%$$

All experiments were performed at least in triplicate. The ANOVA test was used to examine the statistical significance of differences. A p -value less than 0.05 was considered to indicate a statistically significant difference.

2.6 Anti-cercarial activity experiments

Compound **2b** was dissolved in dimethyl sulphoxide (DMSO), and diluted into concentrations with distilled water as follows: 0.6 μM , 1.3 μM , 2.5 μM , 5.0 μM and 10.0 μM . *S. japonicum* cercariae were collected from the infected *O. hupensis*. The *O. hupensis* were induced to shed cercariae by exposing them to bright light for 2 h, and cercariae were then transferred by metal spatula from the water surface to a plate containing a dilute solution of compound **2b**, the activity of the cercariae was explored by biological microscopy at 30 min, 60 min, 90 min and 120 min. The same procedure for **2a**.

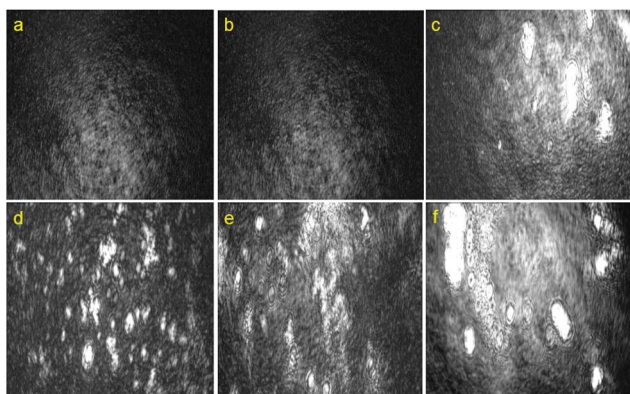


Fig. 1 BAM images the films of compound **2a** with different concentrations at the air–water interface. The morphologies and relative concentrations: (a) black; (b) $7.5 \times 10^{-6} \mu\text{mol cm}^{-2}$; (c) $1.5 \times 10^{-5} \mu\text{mol cm}^{-2}$; (d) $3 \times 10^{-5} \mu\text{mol cm}^{-2}$; (e) $4.5 \times 10^{-5} \mu\text{mol cm}^{-2}$; (f) $7.5 \times 10^{-5} \mu\text{mol cm}^{-2}$.

3. Results and discussions

3.1 BAM images of nano-film pesticides

To observe the morphologies of two novel niclosamide derivatives (compounds **2a** and **2b**) at the air–water interface, BAM images were recorded under different concentration. The concentrations are 0, 7.5×10^{-6} , 1.5×10^{-5} , 3×10^{-5} , 4.5×10^{-5} and $7.5 \times 10^{-5} \mu\text{mol cm}^{-2}$, respectively. Compound **2a** and **2b** could form apparent molecular films at the air–water interface. For compound **2a**, the film cannot be found at low concentration (Fig. 1a and b). With the concentration increasing, white concentric structure appeared while the concentration of compound **2a** is $1.5 \times 10^{-5} \mu\text{mol cm}^{-2}$ (Fig. 1c). It shows that film has emerged. With the further adding of compound **2a**, the concentric structure become denser and more uniform (Fig. 1d and e). It is interesting that concentric structure and banded structure are observed while the concentration of compound **2a** is $7.5 \times 10^{-5} \mu\text{mol cm}^{-2}$ (Fig. 1f). It shows that film has stacked. The film becomes thicker.

Compared Fig. 1 with 2, the concentration of formation film for compound **2b** is lower than that of **2a**. White concentric

structure appeared on the water surface while the concentration of compound **2b** is $7.5 \times 10^{-6} \mu\text{mol cm}^{-2}$ (Fig. 2b). However, white concentric structure cannot be found while the concentration of compound **2a** is $7.5 \times 10^{-6} \mu\text{mol cm}^{-2}$ (Fig. 1b). In addition, white concentric structure of compound **2b** (Fig. 2c and d) is denser and more uniform than **2a** (Fig. 1c and d) at the same concentration. Concentric structure and banded structure (Fig. 2e and f) also appeared on the water surface at $4.5 \times 10^{-5} \mu\text{mol cm}^{-2}$, but banded structures cannot be found at this concentration for compound **2a** (Fig. 1e). The results from BAM revealed that these two derivatives could form self-diffusion thin film at the air–water interface, and the formation ability for films of compound **2b** is better than that of compound **2a**.

3.2 AFM images of nano-film pesticides

These derivatives formed self-diffusion thin film at the air–water interface, but the mechanism of film-forming is not clear. In order to investigate the detailed microcosmic aggregation structures, LB technique has been used at the air–water interface, combined with AFM. Fig. 3 shows the π -A isotherms for the monolayer films of compounds **2a** and **2b** at the air–water interface at 20 °C. The experimental results show two possesses properties of self-diffusion and surface film formation at the air–water interface. When surface pressure less than 35(48) mN m^{-1} , compound **2a** (**2b**) could form stable monolayers on the water surface with a limiting molecular area of around 1.1–2.5 (1.6 – 6.5) nm^2 per molecule, depending on the spacer length, as shown in Fig. 3.

The LB film deposited from the water surface is very flat (Fig. 4 and 5). The AFM height images in Fig. 4 showed planar structures deposited on mica surface from monolayer films of compound **2a** with 0.70 nm, 0.99 nm and 1.50 nm, respectively. The AFM height images in Fig. 5 showed planar structures deposited on mica surface from monolayer films of compound **2b** with 0.85 nm, 1.07 nm and 1.75 nm, respectively. With the increase of surface pressure, the height of the film is larger, which may be attributed to the angle between the niclosamide derivatives and water. Theoretical calculations show that

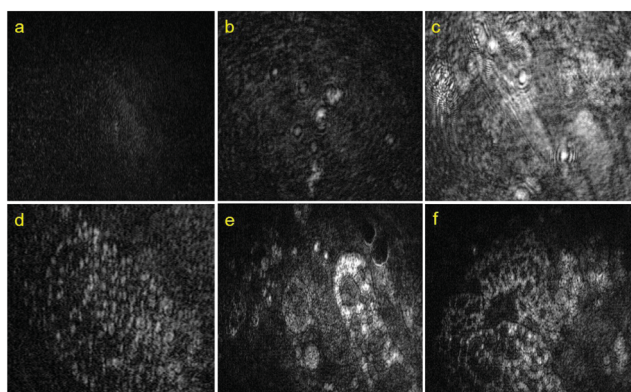


Fig. 2 BAM images the films of compound **2b** with different concentrations at the air–water interface. The morphologies and relative concentrations: (a) black; (b) $7.5 \times 10^{-6} \mu\text{mol cm}^{-2}$; (c) $1.5 \times 10^{-5} \mu\text{mol cm}^{-2}$; (d) $3 \times 10^{-5} \mu\text{mol cm}^{-2}$; (e) $4.5 \times 10^{-5} \mu\text{mol cm}^{-2}$; (f) $7.5 \times 10^{-5} \mu\text{mol cm}^{-2}$.

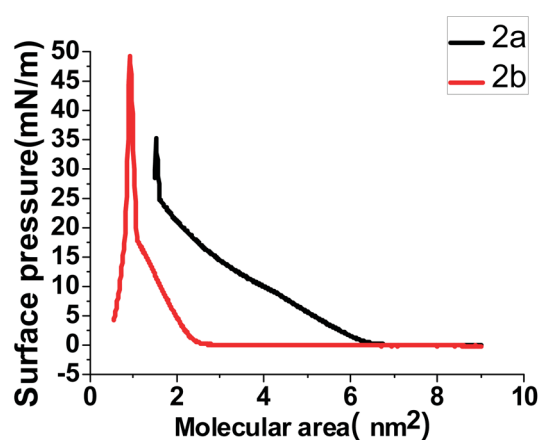


Fig. 3 π -A isotherms for the monolayer films of compounds **2a** and **2b** at the air–water interface at 20 °C.

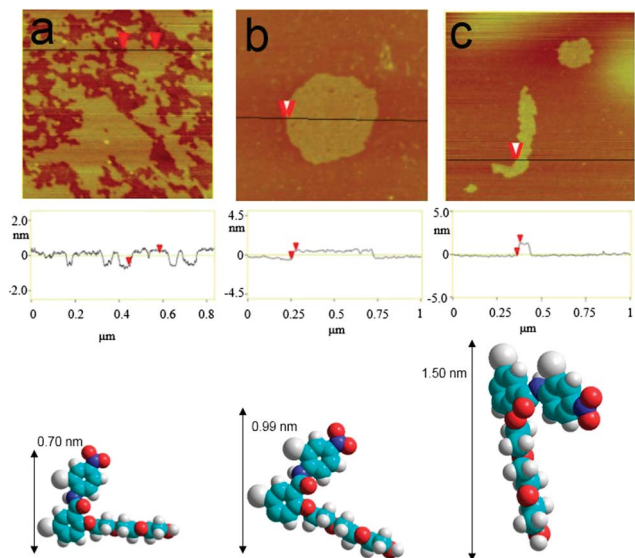


Fig. 4 AFM height images and molecular models of compound **2a** one-layer LB films at different surface pressure. (a) 5 mN m⁻¹, (b) 10 mN m⁻¹, (c) 20 mN m⁻¹, respectively.

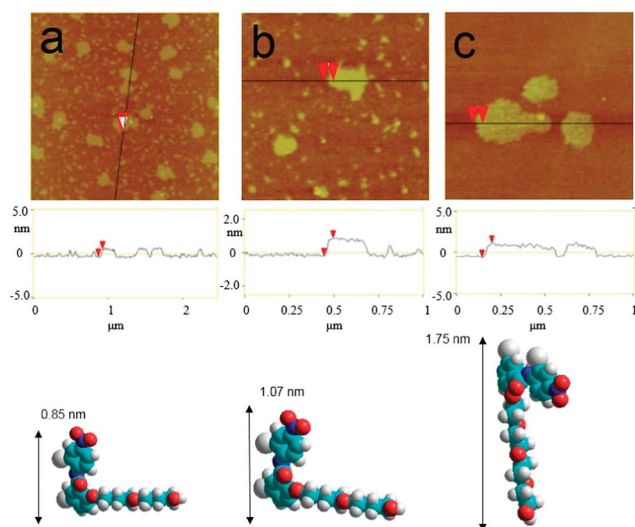


Fig. 5 AFM height images and molecular models of compound **2b** one-layer LB films at different surface pressure. (a) 5 mN m⁻¹, (b) 10 mN m⁻¹, (c) 20 mN m⁻¹, respectively.

niclosamide derivatives nearly lay flat at a surface pressure of 5 mN m⁻¹. With the increase of surface pressure, niclosamide derivatives gradually stand. Niclosamide derivatives nearly totally stand at surface pressure of 20 mN m⁻¹. Under the same surface pressure, the height of compound **2a** film is bigger than compound **2b**. This is due to the hydrophilic group of compound **2a** is longer than compound **2b**.

3.3 Cytotoxicity test

In order to study niclosamide derivatives' cytotoxicity, the MTT assay was used to detect cell survival rate of compound **2a** and

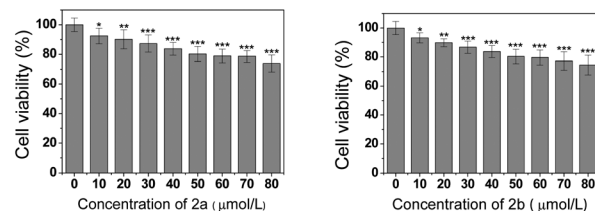


Fig. 6 Cell viability (%) estimated by MTT proliferation test versus incubation concentrations of compound **2a** and **2b**, HeLa cells were cultured in the presence of 0–80 μmol L⁻¹ compound **2a** and **2b** at 37 °C for 24 h. Results are shown as mean ± S.D. of six independent samples (*: $p < 0.05$; **: $p < 0.01$, ***: $p < 0.001$).

Table 1 The mortality rate of *Schistosoma japonicum* cercariae for the cercaricide **2a**^a (25 °C)

Concentration (μM)	Mortality (%)			
	30 min	60 min	90 min	120 min
10.0	100.0	100.0	100.0	100.0
5.0	76.0 ± 1.0	100.0	100.0	100.0
2.5	59.8 ± 3.8	98.6 ± 2.9	100.0	100.0
1.3	0.0	82.2 ± 3.0	93.2 ± 2.7	98.7 ± 1.3
0.6	0.0	61.1 ± 3.4	71.4 ± 2.2	84.4 ± 0.4
Blank	0.0	0.0	0.0	0.0

^a All experiments were performed at least in triplicate.

Table 2 The mortality rate of *Schistosoma japonicum* cercariae for the cercaricide **2b**^a (25 °C)

Concentration (μM)	Mortality (%)			
	30 min	60 min	90 min	120 min
10.0	100.0	100.0	100.0	100.0
5.0	85.2 ± 1.2	100.0	100.0	100.0
2.5	74.6 ± 0.7	100.0	100.0	100.0
1.3	2.8 ± 1.4	90.4 ± 2.4	95.9 ± 0.1	100.0
0.6	0.0	81.0 ± 2.9	86.5 ± 1.9	90.6 ± 2.1
Blank	0.0	0.0	0.0	0.0

^a All experiments were performed at least in triplicate.

2b. Firstly, HeLa cells incubated with **2a** and **2b** for 24 hours, cell viabilities are more than 89% at 20 μM (Fig. 6). With increasing the concentration, the cell survival rate is more than 80% in 50 μM compound **2a** and compound **2b** (Fig. 6).

3.4 Anti-cercarial activity experiments

In order to study anti-cercarial ability of nano-film pesticide, the anti-cercarial activity experiments is performed in different concentration of compound **2a** and **2b**. The mortality rate of *S. japonicum* cercariae for compound **2a** and **2b** was high, not only at a high concentration of 10.0 μM but also at a low concentration of 0.6 μM. Firstly, cercarial incubated with **2a** and **2b** for 30 min, mortality of cercariae are more than 100% at 10.0 μM (Tables 1 and 2). With reducing the concentration, the mortality of cercariae is more than 84% in 0.6 μM compound **2a** and

compound **2b** (Tables 1 and 2). That implies the cercaricide **2a** and **2b** maintained excellent bioactivity against cercariae in spite of the hydroxyl group of niclosamide being replaced by the PEG linker.

4. Conclusion

The niclosamide derivatives have been synthesized and characterized. The BAM experimental results show the niclosamide derivatives can form self-diffusion film at the air–water interface. In order to investigate the detailed microcosmic aggregation structures, LB technique has been used at the air–water interface, combined with AFM. By varying the surface pressure, the nano-film morphologies could be modulated. With the increase of surface pressure, the angles between the niclosamide derivatives and water have changed. Finally, the cell and cytotoxicity experimental results indicated that these two compounds exhibit relatively low cytotoxicity, but have higher efficiency to kill the cercariae compared with that of pristine pesticide.

Acknowledgements

This work was supported by National Science and Technology Ministry (2009BAI78B01, 2009BAI78B02), Jiangxi Province Education Department Science Fund and Jiangxi Provincial Department of Science and Technology Fund.

Notes and references

- 1 J. Chérfas, *Science*, 1989, **246**(4935), 1242.
- 2 Y. Q. Wu, T. S. Yang, X. Li, J. C. Wu, T. Yi, F. Y. Li, C. H. Huang and X. L. Fan, *Dyes Pigm.*, 2011, **88**, 326.
- 3 K. Merschjohann and D. Steverding, *Exp. Parasitol.*, 2008, **118**, 637.
- 4 D. Lowe, J. Y. Xi, X. H. Meng, Z. S. Wu, D. C. Qiu and R. Spear, *Parasitol. Int.*, 2005, **54**, 83.
- 5 B. Devarakonda, R. A. Hill, W. Liebenberg, M. Brits and M. M. Villiers, *Int. J. Pharm.*, 2005, **304**, 193.
- 6 A. Akelah and A. Reha, *Mater. Sci. Eng., C*, 1996, **4**, 1.
- 7 N. Scott and H. Chen, *Nanoscale Science and Engineering for Agriculture and Food Systems*, Cooperative State Research, Education and Extension Service, United States Department of Agriculture, Washington, USA, 2003.
- 8 T. Joseph and M. Morrison, *Nanotechnology in Agriculture and Food*, European Nanotechnology Gateway, 2006, <http://www.nanoforum.org>.
- 9 D. K. R. Robinson and M. Morrison, *Nanotechnology Developments for the Agrifood Sector*, Report of the Observatory NANO, Institute of Nanotechnology, UK, 2009, <http://www.observatorynano.eu>.
- 10 D. F. Emerich and C. G. Thanos, *Expert Opin. Biol. Ther.*, 2003, **3**, 655.
- 11 Y. P. Shi, Z. G. Su, S. Li, Y. N. Chen, X. Chen, Y. Y. Xiao, M. J. Sun, Q. N. Ping and L. Zong, *Mol. Pharmaceutics*, 2013, **10**, 2479.
- 12 H. Zhang, S. Y. Tong, X. Z. Zhang, S. X. Cheng, R. X. Zhuo and H. Li, *J. Phys. Chem. C*, 2007, **111**, 12681.
- 13 K. R. Reddy, *Ann. Pharmacother.*, 2000, **34**, 915.
- 14 S. Bowen, N. Tare and T. Inoue, *Exp. Hematol.*, 1999, **27**, 425.
- 15 A. Gabizon and F. Martin, *Drugs*, 1997, **54**, 15.
- 16 K. J. Harrington, S. Mohammadtaghi and P. S. Uster, *J. Exp. Clin. Cancer Res.*, 2001, **7**, 243.
- 17 E. Johnston, J. Crawford and S. Blackwell, *J. Clin. Oncol.*, 2000, **18**, 2522.
- 18 G. Molineux, O. Kinstler and B. Briddell, *Exp. Hematol.*, 1999, **27**, 1724.
- 19 Y. Q. Shen, E. Jin, B. Zhang, C. J. Murphy, M. H. Sui, J. Zhao, J. Q. Wang, J. B. Tang, M. H. Fan, E. V. Kirk and W. J. Murdoch, *J. Am. Chem. Soc.*, 2010, **132**, 4259.
- 20 J. T. Robinson, G. S. Hong, Y. Y. Liang, B. Zhang, O. K. Yaghi and H. J. Dai, *J. Am. Chem. Soc.*, 2012, **134**, 10664.
- 21 E. B. Watkins, R. J. El-khouri, C. E. Miller, B. G. Seaby, J. Majewski, C. M. Marques and T. L. Kuhl, *Langmuir*, 2011, **27**, 13618.
- 22 S. Kumar and U. Ramachandran, *Tetrahedron*, 2005, **61**, 4141.
- 23 C. P. Mandl and B. Knig, *J. Org. Chem.*, 2005, **70**, 670.